http://www.jgg09.com
Doi:10.3724/SP.J.1246.2010.00008

Simulation of co-seismic gravity change and deformation of Wenchuan *Ms*8.0 earthquake

Chongyang Shen[1,2], Hui Li[1,2] and Hongbo Tan[1,2]
[1] *Institute of Seismology, China Earthquake Administration, Wuhan* 430071, *China*
[2] *Crustal Movement Laboratory, Wuhan* 430071, *China*

Abstract: Surface co-seismic gravity changes and displacements caused by the Wenchuan *Ms*8.0 earthquake are calculated on the basis of the half-space dislocation theory and two fault models inversed, respectively, by Institute of Geophysics, CEA and USGS. The results show that 1) the dislocation consists of dip slip and right-lateral strike slip; 2) the co-seismic gravity change shows a four-quadrant pattern, which is greatly controlled by the distribution of the vertical displacements, especially in the near-filed; 3) the gravity change is generally less than 10×10^{-8} ms^{-2} in the far-field, but as high as several 100×10^{-8} ms^{-2} in the near-filed. These results basically agree with observational results.

Key wards: Wenchuan earthquake; dislocation theory; gravity change; deformation; simulation

1 Introducion

The Wenchuan *Ms*8.0 earthquake that occurred at 14:28 (Beijing time) on May 12, 2008, is located at a secondary fault, the Longmenshan fault, of the most active earthquake-fault zone, the North-South Fault Zone, in Chinese mainland[1]. The Longmenshan fault zone consists of several parallel imbricate thrusts, characterized by a typical thrust nappe structure, and has developed into Wenchuan-Wenmao fault, Beichuan fault, Pengguan fault and Dayi fault from west to east[2]. As indicated by the shrinkage between the north-east and south-west sides of the Songpan-Ganzi fold belt, the nappe probably developed from north-west to south-east, and the fault type evolved from normal to thrust[3-8].

Mobile gravity measurements were made in 1998, 2000, 2002, 2005, 2007 in and nearby the earthquake region by the Crustal-Movement Observation Network and the Digital Earthquake Observation Network of China. Similar measurements were also made by several small local networks in Ganzi, Xichang and Chendu in 1987, 1989 and 1996. Since the earthquake occurrence, we have made two sets of measurement with the local networks. By adopting control with absolute gravity measurement and by adding several temporary stations, we have obtained a relatively large amount of gravity data in the earthquake region.

To clarify the earthquake's development process and the mechanism, it's necessary to analyze and synthesize data and theoretical results obtained from different approaches and points of view. This paper gives a theoretical simulation of the co-seismic gravity and deformation effects, which may be helpful for explaining the development process of the earthquake.

2 Theoretical formula

Based on the elastic dislocation theory[9,10], an earthquake is described as a finite rectangular dislocation in a homogeneous isotropic elastic half-space. For any

Received:2010-07-23; Accepted:2010-09-10
Corresponding author: Tel. -86-27-87667285; E-mail: scy907@163.com
This study was supported by the National Natural Science Fundation of China(40574012)

earthquake, the dislocation is rather complicated, with different amplitudes and directions in different locations of the fault plane. To minimize simulation error introduced by the classical rectangular dislocation, we make use of the idea of fault differentiation and regard a complex fault as a composition of multiple small rectangular faults to approximate a realistic model.

2.1 For a single fault

For a homogeneous rectangular fault (Fig. 1), the gravity change $\Delta\delta$ and deformation Δu on the surface point $(x_1, x_2, 0)$ can be expressed as follows[10]:

$$\Delta g(x_1,x_2) = \{\rho G[U_1 S_g(\xi,\eta) + U_2 D_g(\xi,\eta) + U_3 T_g(\xi,\eta)] + \Delta\rho G U_3 C_g(\xi,\eta)\} \parallel -\beta\Delta h(x_1,x_2) \quad (1)$$

$$\Delta u(x_1,x_2) = \frac{1}{2\pi}[U_1 S(\xi,\eta) + U_2 D(\xi,\eta) + U_3 T(\xi,\eta)] \parallel \quad (2)$$

Where L denotes the length; W, the width; δ, the dip angle; U_1, U_2 and U_3, respectively, the strike slip, the dip slip, and the tensional component; d, the depth to the bottom of the fault; G, the gravitational constant; ρ, the medium density; $\Delta\rho$, the density difference between the media inside and outside the fracture zones; $S_g(\xi,\eta)$, $D_g(\xi,\eta)$, $T_g(\xi,\eta)$, $C_g(\xi,\eta)$, $S(\xi,\eta)$, $D(\xi,\eta)$ and $T(\xi,\eta)$, elastic moduli[9,11]; $\beta = 0.309\times10^{-5}$ m/s^2, the free-air gravity gradient; and Δh, the surface elevation change[9]. The final result in brief form is given below, using Chinnery's notation $\parallel$ to represent substitution.

$$f(\xi,\delta) \parallel = f(x,p) - f(x,p-W) - f(x-L,p) + f(x-L,p-W) \quad (3)$$

Where $p = y\cos\delta + d\sin\delta$ (4)

2.2 For multiple faults

Assuming a surface coordinate system O-XYZ (X axis pointing to the east, Y axis to the north, and Z axis is downward), where $S(s_x, S_y, 0)$ is the midpoint of the surface trace (or projection line) of the fault (fig. 2), and is the fault's azimuth, the gravity change and deformation on a surface point (x, y, o) can be expressed

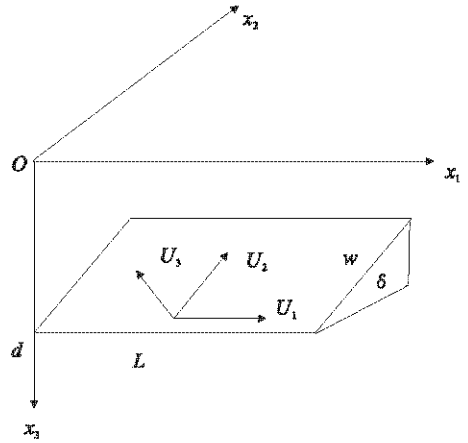

Figure 1 Dislocation model for a rectangle fault

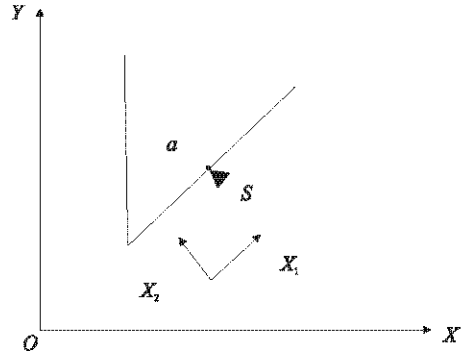

Figure 2 Surface coordinate system for fault movement

as the superposition of several faults:

$$\Delta G = \sum_{i=1}^{N} \Delta g_i(x,y,0;U_1,U_2,U_3,L,W,d,\delta,\alpha,s_x,s_y) \quad (5)$$

$$u = \sum_{i=1}^{N} \Delta u_i(x,y,0;U_1,U_2,U_3,L,W,dt,\delta,\alpha,s_x,s_y) \quad (6)$$

From the above relations, it may be seen that the surface gravity change and deformation are related to the component faults' dimension, position, altitude and dislocation. The superposition of the effects of all the component faults gives the simulated gravity change and deformation, which are enhanced if the components have the same signs, and reduced, if otherwise.

3 Fault models

The dislocation-model parameters of slip distribution along the seismogenic-fault plane are determined mainly from the analysis of seismic data. Shortly after the Wenchuan earthquake, groups of scientists in China, America and Japan inversed the earthquake-rupture

process from seismic data, and published the results on the internet[1,13]. The different results are basically consistent with one another, showing that the faulting consists of mainly a dip slip and secondarily a right-lateral strike slip. This feature is in agreement with the characteristics of Longmenshan fault and the distribution pattern of the aftershocks. Here we have chosen to use two results, given by the Institute of Geophysics, China Earthquake Administration (IGCEA) and the United States Geological Survey (USGS).

3.1 The IGCEA model

In this model, which is inversed by Chen Yuntai, Xu Lisheng, et al[1], the fault plane and the slip are in the same direction. The distribution of static dislocation in the fault plane is shown in Fig. 3 (The large white angular symbol indicates the location of hypocenter and the white circles, the aftershocks projected on the fault

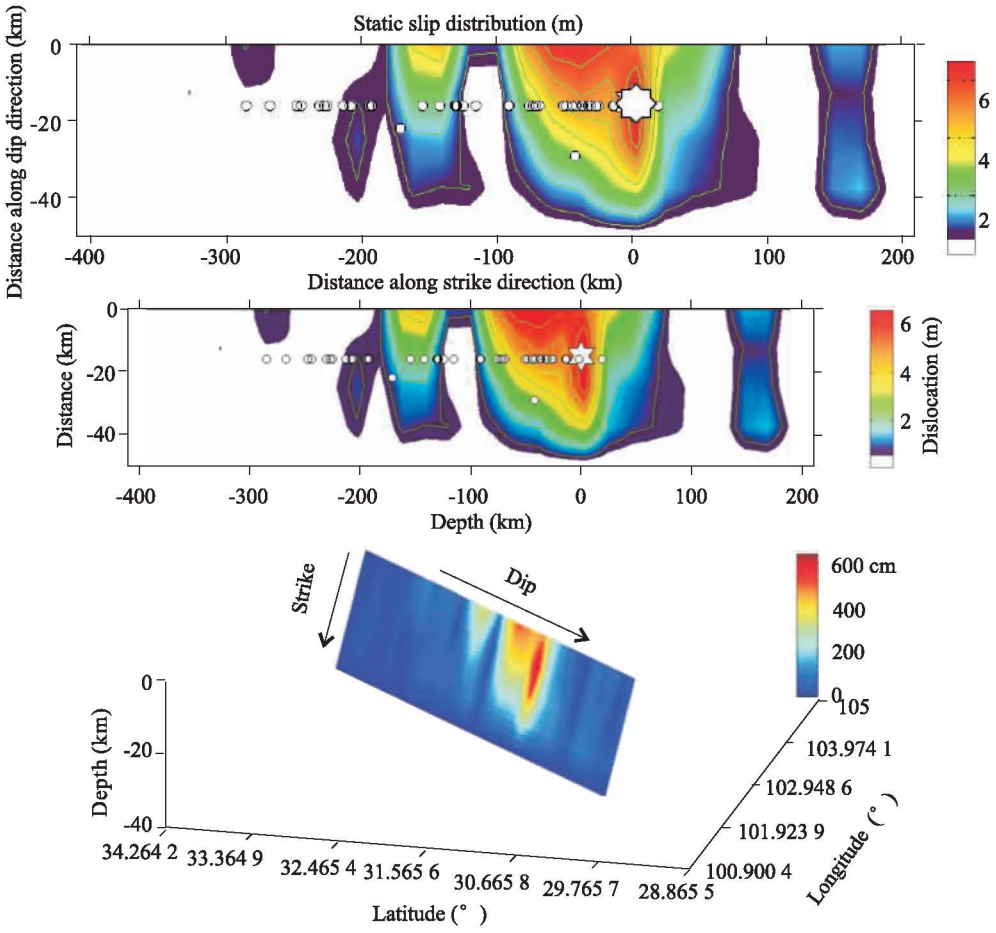

Figure 3 The distribution of static dislocation on the fault plane (IGCEA model)

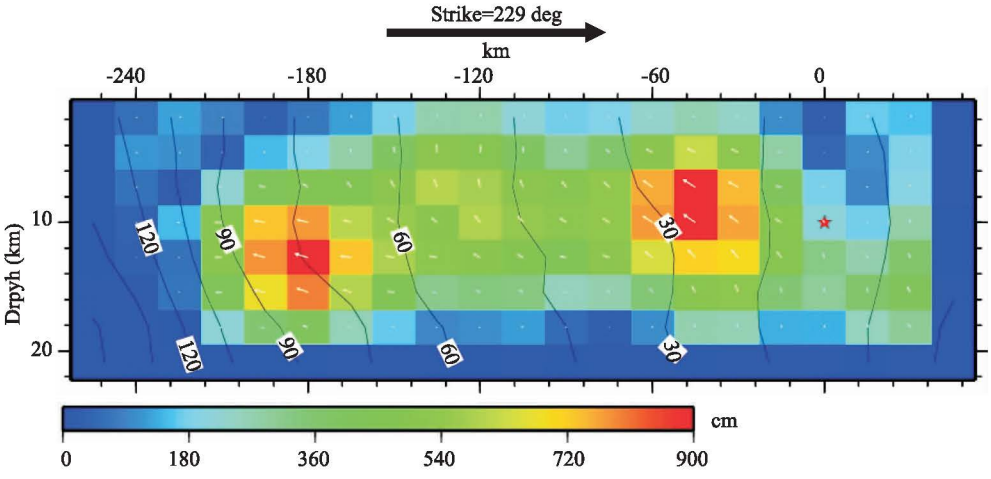

Figure 4 The cross section of the seismogenic fault, including movement distribution

plane). The maximum static displacement on the fault is 6.7 m, whereas the average value is 1.5 m. The composite fault parameters we used are as follows: The strike is 230°; dip angle, 39°; slip angel, 120°; the fault is represented by 31 × 5 sub-faults along the strike and dip, and each sub-fault is 20 km × 10 km in dimension.

3.2 The USGS model

In this model, which is inversed by Chen Ji (UCSB) and Gavin Hayes (NEIC), the slip direction is not in the fault plane (Fig. 4). Red star represents the epicenter; different colors indicate different amounts of slip; arrow, movement direction of hanging wall relative to footwall; dark lines, rupture times). The optimum fault parameters are as follows: strike, 229°; dip angle, 33°; number of sub-faults, 21 × 8 blocks along strike and dip, respectively; and each sub-fault, 15 km × 5 km.

4 Simulated surface co-seismic gravity change

Our simulation covers the region of 99° – 107° E and 28° – 36° N, with a grid size of 0.025° × 0.025°, in accordance with the coverage of the regional gravity network.

4.1 IGCEA – model result

The surface gravity change calculated with IGCEA model (Fig. 3) and the theoretical formula is shown in Fig. 5 (a). The co-seismic gravity change exhibits a symmetric four-quadrants pattern. In the far-field, the gravity change is negative in the northwest and southeast quadrants, and positive in the northeast and southwest quadrants. In the near-field, zones of opposite signs appear alternately in space, with extreme values of -530×10^{8} ms^{-2} and $+110 \times 10^{-8}$ ms^{-2}.

4.2 USGS-model result

The co-seismic gravity change calculated with the USGS model (Fig. 4) is shown in Fig. 5 (b). Comparing with Fig. 5 (a), it may be seen that the characteristics are basically the same, except a small difference in amplitude range (most in the near field); the extreme values in this case are about -420×10^{-8} ms^{-2} and $+80 \times 10^{-8}$ ms^{-2}.

5 Simulated surface deformation

In order to better understand the characteristics of the co-seismic gravity changes, the co-seismic surface deformations caused by the above rupture models were calculated also (Fig. 6). Fig. 6 shows that the simulation results obtained with the two different models basically have the same displacement pattern, but a significantly different amplitude range in the near field (these differences are caused by the difference between the fault models; for example, the IGCEA model breaks through the earth's surface whereas the USGS model doesn't; the IGCEA model's length is obviously longer than that of the USGS model.)

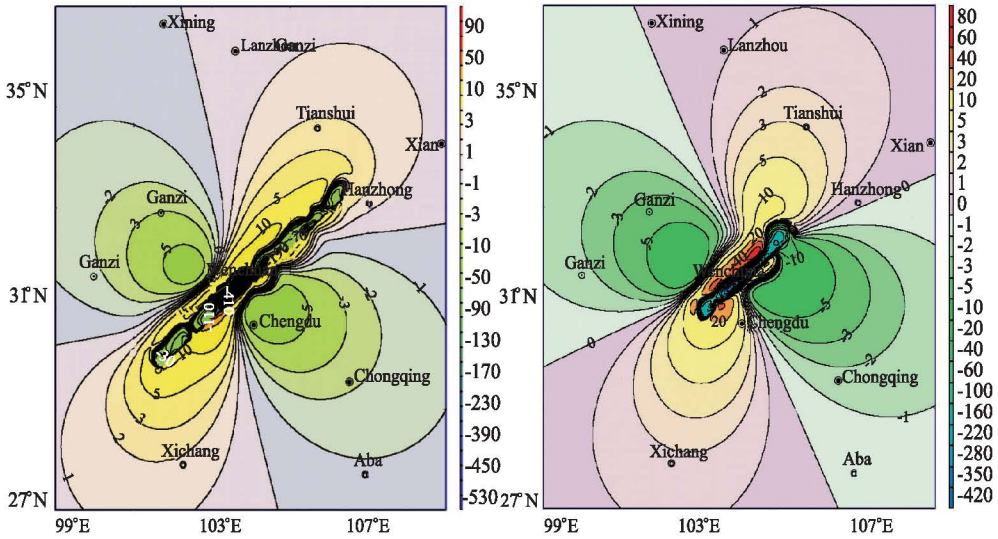

Figure 5 Co-seismic surface gravity changes caused by the fault dislocation of Wenchuan *Ms*8.0 earthquake (left: IGCEA; right: USGS; unit: 10^{-8} ms^{-2})

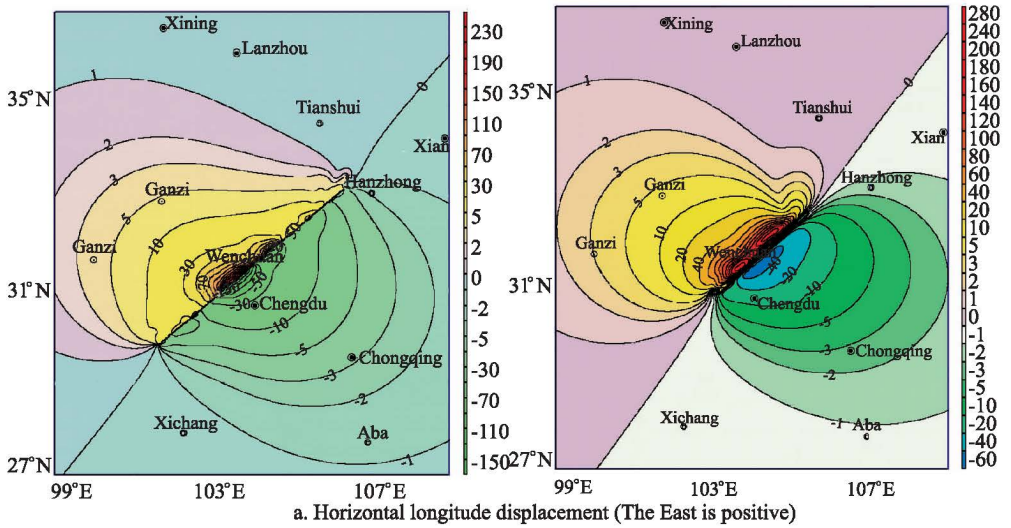

a. Horizontal longitude displacement (The East is positive)

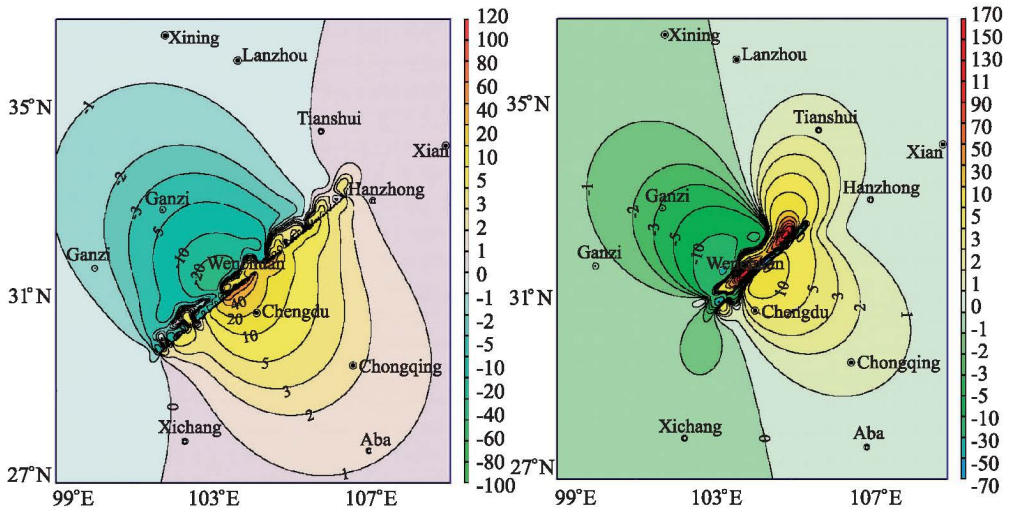

b. Horizontal latitudinal displacement (The North is positive)

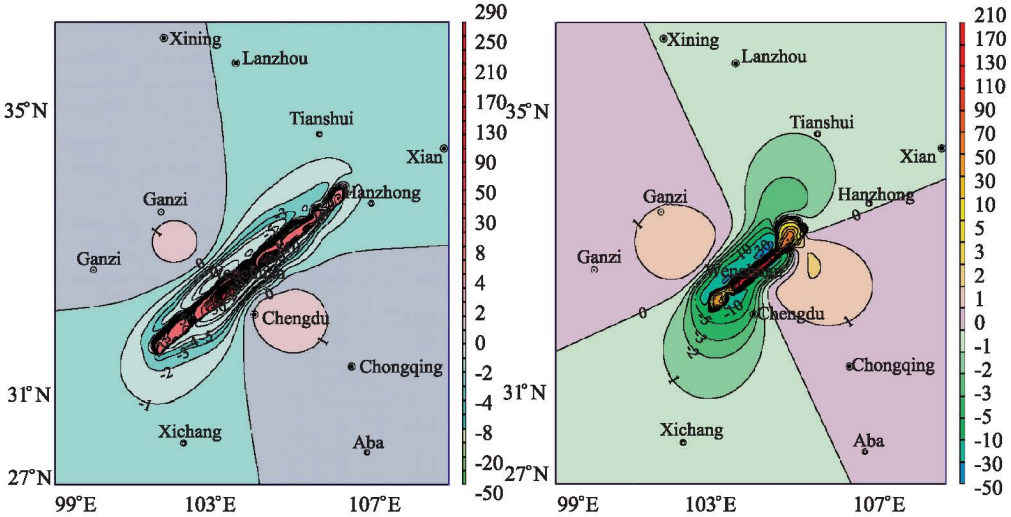

c. Vertical displacement (The Upward is positive)

Figure 6 Co-seismic surface deformation caused by Wenchuan *M*s8.0 earthquake (left, IGCEA model; right USGS model; unit: cm)

The pattern of horizontal longitudinal displacement (Fig. 6(a)) is divided into northwestern and southeastern areas, bordering along the rupture zone. The iso-displacement lines are symmetric, with positive values in northwest area (upper wall of the fault has an eastward thrust component), and negative values in the southeast area (bottom wall has a westward dive component). The amplitude decreases rapidly with epicentral distance in the near field (IGCEA model: -50 – -150 cm, $+70$ – $+250$ cm; USGS model: -40 – -60 cm, $+60$ – $+280$ cm), but slowly in the far field.

The pattern of horizontal latitudinal displacement (Fig. 6(b)) is divided also into northwestern and southeastern areas, bordering along the rupture zone. The iso-displacment lines show certain symmetry, but the two models' results are a little more different. In the northwestern area, the values are negative; the upper wall of the fault has a southward thrust component, while the bottom wall has a northward dive component. The amplitude decreases rapidly with epicentral distance in the near field (IGCEA model: -20 – -100 cm, $+20$ – $+120$ cm; USGS model: -30 – -70 cm, $+30$ – $+170$ cm), but slowly in the far field. The differences between the two results are mainly that, relative to the IGCEA result, the lines in the USGS result shrink toward the seismogenic rupture area, and the lines in the southeastern area is rotated 60 degrees counter-clockwise.

The pattern of vertical displacement (Fig. 6(c)) is also divided into northwestern and southeastern areas. The iso-displacement lines are symmetric, and the amplitude changes mainly in the near field (IGCEA model: -5 – -50 cm, $+10$ – $+290$ cm; USGS model: -10 – -50 cm, $+10$ – $+210$ cm), but very little in the far field (0 – 10 cm). The vertical displacement is positive (uplift) along the fault in the middle of the near field, but decreases rapidly to zero and then becomes negative in the surrounding area. By comparing with the pattern of surface gravity changes, one may see that the near-field gravity changes are mainly affected by vertical surface displacement.

6 Analysis and conclusion

1) The co-seismic gravity changes from the simulation studies show that the earthquake faulting consists of mainly dip slip and secondarily right-lateral strike slip. The co-seismic gravity changes in the far-field show a symmetric four-quadrant distribution bordered along the fault. The changes in northwest and southeast quadrants are negative, whereas those in the northeast and southwest quadrants are positive. The amount of changes is generally less than 10×10^{-8} ms^{-2}. However, in the near-field, the changes are large in zones of opposite signs that appear alternately in space.

2) The co-seismic deformations calculated with the two different models are similar. The near-field vertical deformation has a significant effect on the gravity change, whereas the horizontal surface deformation does not.

3) Our simulation result is in good agreement with that of Chen Yuntai, Xu Lisheng, et. al[1], who have simulated the surface deformation in a homogeneous elastic half-space, indicating the reliability and reasonableness of our result.

4) To compare with the actually observed data, Table 1 lists both the simulation results and the absolute gravity and GPS results observed at the Pixian station (103.7°E, 30.91°N). The simulation results based on the IGCEA model are generally close to the observed results in gravity change, latitudinal deformation and vertical deformation, but much different in longitudinal deformation. But the results based on USGS model are quite different from the observed results. This may suggest that the IGCEA model is more realistic. Currently, earthquake rupture models are mainly inversed from seismic data, and are not unique. To reduce this non-uniqueness, the use of co-seismic gravity change and deformation to check the rupture models may prove to be a worthwhile research effort.

5) It is fairly obvious that the earthquake has introduced significant density changes in the underground media. Our simulation results indicate that, by using USGS model, the co-seismic gravity change and vertical deformation at the Chendu-Pixian station are, respectively, 23.0×10^{-8} m/s^2 (decrease) and -9.1 cm (sink, which is equivalent to a gravity change of -5.1×10^{-8} m/s). This indicates a co-seismic

Table 1 Comparison between simulation and actually observed results at the Pixian station

	Gravity change (1×10^{-8} ms^{-2})	Lonsitudianl deformation (cm)	Latitudinal deformation (cm)	Vertical deformation (cm)
CEA mdoel	2.4	49.4	34.3	2.9
USGS model	23.0	-21.2	2.4	-9.1
Absolute gravity[14]	0.0±2.5	-	-	-
GPS	-	-56.4±0.14	42.6±0.13	0.53±0.25

gravity change of -5.1×10^{-8} m/s^2 caused by underground medium change. By using the IGCEA model, these changes are, respectively, 2.4×10^{-8} m/s^2 (increase) and 2.9 cm (uplift, which is equivalent to a gravity change of -8.9×10^{-8} m/s^2), indicating a co-seismic gravity change of 11.3×10^{-8} m/s^2 caused by underground medium change.

6) The preliminary results of regional mobile gravity surveys made before and after the earthquake indicate a four-quadrants pattern of the actual gravity changes. Compared with the similar patterns of the simulating results, it is different in orientation, and amplitude. The difference might be due to the survey-station distribution and several other factors. The simulation is only for a case of instantaneous effect of an elastic dislocation, whereas the actual results were obtained during a longer period and thus might be affected by many factors, including not only co-seismic, but also pre-earthquake (about one year) and post-earthquake (about 10 days) gravity changes, involving non-seismic effects (for example, mass transport).

7) Because of the simplicity of the theoretical models, which have not taken into account the heterogeneity and viscoelastic property of materials at depth, the simulation results are bound to be somewhat inaccurate. However, the basic features are probably credible, and may be used as a reference for studying the mechanism of the Wenchuan earthquake.

References

[1] Chen Yuntai, et al. Analysis report about the hypocenter characteristic of the Wenchuan earthquake happened on 5 12th 2008. China Seismic Information Net (http://www. csi. ac. cn/sichuan/), 2008, 5. (in Chinese)

[2] Li Yong, Zhou Rongjun, Densmore A L and Ellis M A. Geomorphic evidence for the late Cenozoic strike-slipping and thrusting in Longmenshan at the eastern margin of the Tibetan Plateau [J]. Quaternary Sciences, 2006, 26(1): 40 - 51. (in Chinese)

[3] Zhou Rongjun, et al. Active tectonics of the eastern margin of the Tibet Plateau [J]. J Mineral Petrol, 2006, 26(2): 40 - 51. (in Chinese)

[4] Bai Lanxiang, Wen Xueze. Seismic potential of Long-term strong shock on the Maowen-Wenchuan segment of the Longmenshan fault zone[J]. Sichuan Earthquake, 1994, 3: 51 - 58. (in Chinese)

[5] Alexander L, et al. Active tectonics of the Beichuan and Pengguan faults at the eastern margin of the Tibetan Plateau[J]. Tectonics, 2007, 26, TC4005: 1 - 17.

[6] An Qimei, Ding Lifeng, Wang Haizhong and Zhao Shiguang. Research of property and activity of Longmenshan fault zone[J]. Journal of Geodesy and Geodynamics, 2002, 32(2): 68 - 74. (in Chinese)

[7] Jiao Qing, et al. Preliminary study on motion characteristics of Longmenshan fault before and after *Ms*8.0 Wenchuan earthquake [J]. Journal of Geodesy and Geodyamics, 2008, 28(4): 7 - 12. (in Chinese)

[8] Tang Wenqing, et al. GPS study on Longmenshan fault zone[J]. Journal of Geodesy and Geodynamics, 2004, 24(3): 57 - 59. (in Chinese)

[9] Okada Y. Surface deformation due to shear and tensile faults in half-space[J]. Bull. Seism. Soc. Am., 1985, 75: 1 135 - 1 154.

[10] Okubo S. Gravity and potential changes duo to shear and tensile faults in a half - space[J]. JGR, 1992, 97(B5): 7 134 - 7 144.

[11] Okubo S. Potential and gravity changes raised by point dislocations[J]. Geophys J Int., 1991, 105: 573 - 586.

[12] Tan Hongbo, Shen Chongyang and Li Hui. The characteristic of surfer gravity changes caused by a fault or faults dislocation[J]. Journal of Geodesy and Geodynamics, 2008, 28(4): 54 - 62. (in Chinese)

[13] Chen Ji, UCSB and Gavin Hayes, NEIC. Preliminary result of the May 12, 2008 Mw7.9 eastern Sichuan, China earthquake, http://earthquake. usgs. gov/eqcenter/eqinthenews/ us2008ryan/. 2008.5.

[14] Xing Lelin, et al. Analysis of repeat absolute gravity surveying results at Chendu earthquake station[J]. Journal of Geodesy and Geodynamics, 2008, (6): 38-42. (in Chinese)